AD-A172 317 REGIONAL STUDIES WITH BROADBAND DATA(U) CALIFORNIA UNIV 1/1
BERKELEY DEPT OF GEOLOGY AND GEOPHYSICS
T V MCEVILLY ET AL. 06 JUN 86 TR-1 AFGL-TR-86-0124
UNCLASSIFIED F19628-85-K-0025 F/G 8/13 NL

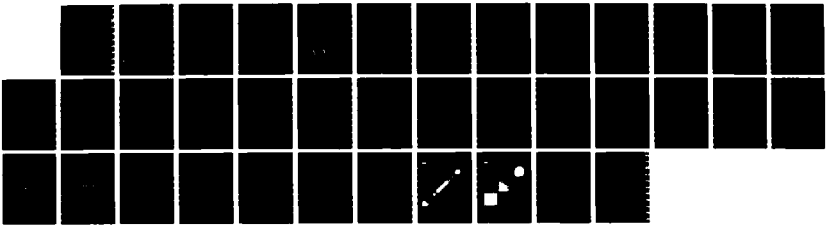

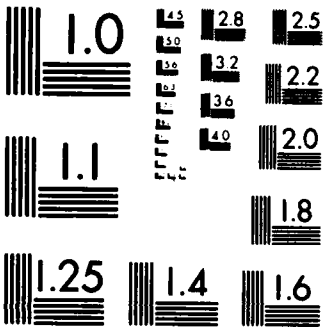
1.0
1.1
1.25
1.4
1.6
1.8
2.0
2.2
2.5
2.8
3.2
3.6
4.0
4.5
5.0
5.6

AD-A172 317

13

AFGL-TR-86-0124

Regional Studies With Broadband Data

Thomas V. McEvilly
Lane R. Johnson

University of California
Geology and Geophysics
Berkeley, CA 94720

6 June 1986

Semiannual Report No. 1

APPROVED FOR PUBLIC RELEASE; DISTRIBUTION UNLIMITED

DTIC
ELECTE
SEP 2 3 1986
S D
B

DTIC FILE COPY

AIR FORCE GEOPHYSICS LABORATORY
AIR FORCE SYSTEMS COMMAND
UNITED STATES AIR FORCE
HANSCOM AIR FORCE BASE, MASSACHUSETTS 01731

86 9 23 055

CONTRACTOR REPORTS

This technical report has been reviewed and is approved for publication.

JAMES F. LEWKOWICZ
Contract Manager

HENRY A. OSSING
Chief, Solid Earth Geophysics Branch

FOR THE COMMANDER

DONALD H. ECKHARDT
Director
Earth Sciences Division

This report has been reviewed by the ESD Public Affairs Office (PA) and is releasable to the National Technical Information Service (NTIS).

Qualified requesters may obtain additional copies from the Defense Technical Information Center. All others should apply to the National Technical Information Service.

If your address has changed, or if you wish to be removed from the mailing list, or if the addressee is no longer employed by your organization, please notify AFGL/DAA, Hanscom AFB, MA 01731-5000. This will assist us in maintaining a current mailing list.

Unclassified

SECURITY CLASSIFICATION OF THIS PAGE

A172 317

REPORT DOCUMENTATION PAGE

1a. REPORT SECURITY CLASSIFICATION: Unclassified	1b. RESTRICTIVE MARKINGS:
2a. SECURITY CLASSIFICATION AUTHORITY:	3. DISTRIBUTION/AVAILABILITY OF REPORT: Approved for public release; Distribution unlimited
2b. DECLASSIFICATION/DOWNGRADING SCHEDULE:	
4. PERFORMING ORGANIZATION REPORT NUMBER(S): TR-1	5. MONITORING ORGANIZATION REPORT NUMBER(S): AFGL-TR-86-0124
6a. NAME OF PERFORMING ORGANIZATION: University of California; 6b. OFFICE SYMBOL (If applicable):	7a. NAME OF MONITORING ORGANIZATION: Air Force Geophysics Laboratory
6c. ADDRESS (City, State and ZIP Code): Geology and Geophysics, University of California, Berkeley, California 94720	7b. ADDRESS (City, State and ZIP Code): Hanscom Air Force Base, Massachusetts 01731
8a. NAME OF FUNDING/SPONSORING ORGANIZATION: DARPA; 8b. OFFICE SYMBOL (If applicable): DARPA/GSD	9. PROCUREMENT INSTRUMENT IDENTIFICATION NUMBER: F19628-85-K-0025
8c. ADDRESS (City, State and ZIP Code): 1400 Wilson Blvd., Arlington, Virginia 22209	10. SOURCE OF FUNDING NOS: PROGRAM ELEMENT NO. 61101F; PROJECT NO. 5A10; TASK NO. DA; WORK UNIT NO AC
11. TITLE (Include Security Classification): Regional Studies with Broadband Data	
12. PERSONAL AUTHOR(S): McEvilly, Thomas V., Johnson, Lane R.	
13a. TYPE OF REPORT: Semi-Annual Report 1; 13b. TIME COVERED: FROM 2/13/85 TO 9/30/85; 14. DATE OF REPORT (Yr., Mo., Day): 6/6/86; 15 PAGE COUNT: 38	
16 SUPPLEMENTARY NOTATION: (Seismic waves, Seismic data ?)	

17 COSATI CODES		
FIELD	GROUP	SUB GR

18 SUBJECT TERMS (Continue on reverse if necessary and identify by block number): Nuclear explosion, Velocity structure, Nevada Test Site

19. ABSTRACT (Continue on reverse if necessary and identify by block number)

A laterally averaged one dimensional P and S wave velocity stucture is obtained for Silent Canyon Caldera, located beneath Pahute Mesa at the Nevada Test Site. The velocity models are derived from a linearized damped least squares travel time inversion for slowness gradient perturbations. A total of 72 P wave and 20 S wave travel times generated from 13 different explosions, and obtained at scattered locations above the caldera, are used in the inversion. The structure is modeled using linear velocity gradients. The inversion produces a model which increases in velocity from 1.50 km/sec at the surface to 4.62 km/sec at 2.5 km depth for P waves, and from 0.99 km/sec at the surface to 2.35 km/sec at 2.5 km depth for S waves. The P and S wave models produce travel time residuals which are typically less than 0.1 and 0.2 seconds, respectively, which is within observational error. However, P wave amplitude ratios and waveform characteristics of data collected from 7 explosions buried near 625 m depth indicate the presence of lateral variations within the caldera which may be significant to nuclear source studies. Requests

20 DISTRIBUTION/AVAILABILITY OF ABSTRACT: UNCLASSIFIED/UNLIMITED X SAME AS RPT. DTIC USERS	21 ABSTRACT SECURITY CLASSIFICATION: Unclassified	
22a NAME OF RESPONSIBLE INDIVIDUAL: James F. Lewkowicz	22b TELEPHONE NUMBER (Include Area Code): (617) 377-3128	22c OFFICE SYMBOL: AFGL/LWH

DD FORM 1473, 83 APR

Contributing Scientists

The following scientists contributed to the research performed during the period covered by this report:

T. V. McEvilly	Professor of Seismology
L. R. Johnson	Professor of Geophysics
M. A. Leonard	Graduate Student
M. E. Templeton	Graduate Student
D. R. O'Connell	

DTIC
ELECTE
SEP 2 3 1986
S D
B

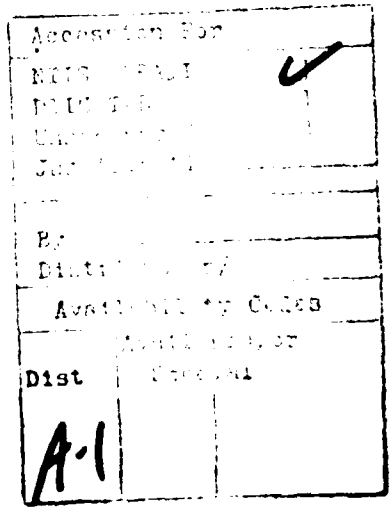

QUALITY INSPECTED 4

Velocity Structure of Silent Canyon Caldera, Nevada Test Site

Michael A. Leonard and Lane R. Johnson

Center for Computational Seismology, Lawrence Berkeley Laboratory
and
Department of Geology and Geophysics, University of California
Berkeley, CA 94720

ABSTRACT

A laterally averaged one dimensional P and S wave velocity structure is obtained for Silent Canyon Caldera, located beneath Pahute Mesa at the Nevada Test Site. The velocity models are derived from a linearized damped least squares travel time inversion for slowness gradient perturbations. A total of 72 P wave and 20 S wave travel times generated from 13 different explosions, and obtained at scattered locations above the caldera, are used in the inversion. The structure is modeled using linear velocity gradients. The inversion produces a model which increases in velocity from 1.50 km/sec at the surface to 4.62 km/sec at 2.5 km depth for P waves, and from 0.99 km/sec at the surface to 2.35 km/sec at 2.5 km depth for S waves. The P and S wave models produce travel time residuals which are typically less than 0.1 and 0.2 seconds, respectively, which is within observational error. However, P wave amplitude ratios and waveform characteristics of data collected from 7 explosions buried near 625 m depth indicate the presence of lateral velocity variations within the caldera which may be significant to nuclear source studies.

Introduction

The Silent Canyon Caldera, located within Pahute Mesa in the north-west corner of the Nevada Test Site, has been and continues to be the site of numerous underground nuclear detonations. The ground motion recordings generated by these explosions provide the necessary data for a study of the physics of the explosive source as a generator of seismic energy. When inferring properties of the seismic source from observed ground motion, one is faced with a fundamental problem of seismology, namely that the net recorded motion represents a coupling between the source signature and the response to the physical structure through which the seismic energy propagates. To accurately determine the characteristics of the source, the velocity, density, and attenuation structure must be known. The intent of this study is to estimate an improved shallow velocity structure of Silent Canyon Caldera in the hopes that seismic sources generated there may be better resolved in subsequent studies of ground motion data.

There have been a number of published velocity models for Pahute Mesa, e.g., Carrol (1966), Hamilton and Healy (1969), Helmberger and Hadley (1981), Hartzell, et al. (1983), and Stump and Johnson (1984). These models are based primarily on a limited amount of drill hole and travel time data. The velocity model to be presented in this paper uses a much larger set of travel times in a linearized inversion for slowness gradient perturbations from an initial model. Additionally, a suite of near-field waveform data have been analyzed for indications of coherent reflectors within the caldera. These data have been collected at more or less random locations above the caldera (Figures 1a and 1b). Reflection or refraction surveys specifically aimed at elucidating the two or three-dimensional structure of the caldera have not yet been attempted. Therefore, in the absence of a more extensive data set, we will offer a one dimensional velocity structure

which averages through any lateral variations. Previous velocity models have likewise made this simplification. In an attempt to assess the validity of this approximation, we will qualitatively examine the possible effect of lateral heterogeneity on the suite of waveform data. Following this will be the results of the one dimensional travel time inversion.

Geologic Setting and Lateral Heterogeneity

The Silent Canyon Caldera is located within a pyroclastic volcanic center located in the eastern portion of Pahute Mesa. The center was volcanically active for at least 1 m.y. in the late Miocene (13.1 - 14.8 m.y.) during which time it collapsed and became partially filled with self-derived tuffs and lava flows (Noble, et. al. 1968). Subsequent to the collapse and general volcanic activity, the caldera became almost completely buried with volcanics erupted from younger nearby centers. The surface outline of the caldera shown in Figures 1a and 1b is for the most part inferred from gravity, surface geological mapping, and subsurface data.

The availability of limited borehole data throughout the caldera has made it possible for geologists to construct stratigraphic profiles. Volcanic sediments have been locally mapped down to 4 km depth. The overall interpretation by Orkild, et. al. (1968) indicates three basic types of structural lateral heterogeneities. These are (1) an abundance of basin and range normal faulting, (2) interfingering of rock units, and (3) non-uniform collapse of the caldera itself. These structural variations are reflected in down hole density measurements which vary from about 1.9 to 2.5 gm/cc at a given depth down to at least 1.5 km among boreholes throughout the caldera (Healy, 1968).

Our one-dimensional model cannot deal with such irregularities. However, in seismic source studies it is important to at least qualitatively understand the effect of lateral heterogeneities on waveform data. To this end, we now consider the near field ground motion data from seven explosions, each buried near 625 m depth, and examine the effect that lateral variations may have on these data. Combining explosions with similar source depths allows us to interpret the waveforms as if they were all generated from a single source. The explosions used here are Chancellor, Colwick, Emmenthal, Farm, Harzer, Pipkin, and Serpa (see Figure 1a. and Table 1a). Most stations recorded all three components of ground acceleration, yielding a total of 44 recordings per component. The recordings from these scattered stations are contracted onto a one-dimensional line and plotted in Figures 2 to 4 as a function of distance away from their respective explosion. Each trace is normalized to its own maximum amplitude. For reasons to be discussed later, the traces have been shifted slightly in time.

The actual first arrival times of these waveforms, as measured off the vertical component, are plotted in Figure 5. A fair amount of scatter is evident, ranging up to 0.3 seconds. If the caldera were laterally homogeneous, then the scatter of points could only be due to timing inaccuracies. We estimate the instrumental timing errors of these data to be typically no greater than about 0.05 seconds, though the scatter in the Colwick times suggests possible timing errors up to a tenth of a second. The picking error is typically about 0.01 seconds for these P arrivals. The scatter may also in part be due to differences in station elevations. The average height of the stations above the elevation of the lowest station is 132 m, the maximum being 225 m. For a near surface velocity of 1.5 km, this would result in relative delay times of a tenth of a second or so. However, an attempt to correct the travel times to a common datum did not reduce the scatter by any significant amount. The scatter of these travel times beyond the total timing and picking

error of 0.11 seconds thus suggests that there exist lateral velocity variations capable of generating travel time anomalies up to a few tenths of second. The ray bottoming depths for these scattered arrivals, as determined from our final model, suggest that such heterogeneities are present down to a depth of at least 2.5 km, consistent with the geologic interpretation.

An additional indication of lateral heterogeneity is the variation in the ratio of P wave vertical amplitude, A_V, to P wave radial amplitude, A_R. If the media were laterally homogeneous and each of the seven explosions generated similar source pulses, one would expect similar variations of A_V/A_R as a function of epicentral distance. The P wave acceleration amplitude ratios for these data, as measured off the first quarter cycle, are given in Figure 6. Significantly different patterns of A_V/A_R between explosions are apparent. This is an indication that waves travelling the same epicentral distance, but in different parts of the caldera, may be sampling substantially different velocities along their paths.

Some degree of this disparity between explosions may also be due to topographic focussing effects. Additionally, many of the stations recorded transverse motion arriving coincident with the first half cycle of the P arrival on the two isotropic components, i.e., the radial and vertical components (see Figure 4). The amplitudes of these arrivals are often a few tens of percent of the vertical P wave amplitude and even as large as 95 % at one of the Farm stations. These transverse arrivals may be indicative of lateral diffraction and/or scattering of energy, both of which may affect the P wave amplitudes on the vertical and radial components of ground motion. Though the implications of the amplitude data are not entirely conclusive, some observable degree of lateral inhomogeneity in the structure is indicated.

Our final comments on the subject of lateral heterogeneity within the caldera are directed at the waveforms themselves. By combining the traces into record sections, as in Figures 2 to 4, our intent was to search the suite of seismograms for indications of subsurface structure, i.e., reflections passing coherently through the sections. The problem of static time corrections was best solved by fitting a smooth curve through the scattered P travel times in Figure 5 and shifting the traces on all three components by the amount necessary to align the vertical P wave onsets with the smooth curve. The curve was initially generated in a trial and error fashion by numerically calculating the P wave travel times for various preliminary velocity models. The model which appeared to best average through the data also served as the initial velocity model for the linearized inversion. In an attempt to align later arrivals in the sections as best as possible, the first arrivals were shifted to coincide with the predicted P wave travel times from our final model, as shown in Figure 5.

Though reflection hyperbolas are not clearly evident, the sections do show some coherency between the traces recorded at the closely packed Colwick and Serpa stations. In an attempt to extract some amount of structural detail from such coherency, the sections were subjected to some of the standard processing techniques that are applied to controlled source reflection data. For example, the traces were filtered at various bandpasses and examined for reflections using a velocity spectra technique, (Taner and Koehler, 1969). However, no definitive reflecting horizons were uncovered in this process. This may in part be due to negligible acoustic impedance contrasts across stratigraphic units. However, the overall non-coherency between events and within non-array recorded events suggests that the waves have traveled through and have been reflected off different lateral heterogeneities within the caldera. The presence of near surface heterogeneities are suggested by the non-uniformity of surface waves across the sections.

These waveform data, as well as P wave travel times and amplitude measurements, are fairly strong indicators that lateral variations of structure within Silent Canyon Caldera may be significant. However, without good quality reflection or refraction data, one must settle for an averaged one dimensional velocity model.

Travel Time Inversion

In an attempt to make more quantitative use of the available travel times, we have implemented a least squares travel time inversion. Given an initial velocity model reasonably close to the true model, one can make use of travel time data to refine the model parameters, bringing them closer to a model which better fits the travel times. Work by Backus and Gilbert (1969) and Pavlis and Booker (1980) describe the method of velocity model refinement in detail and apply it to earthquake travel time data. In our study, using only explosion data, we have the advantage that locations and origin times are known and need not be solved for in the inversion. The problem is then simplified and is outlined below.

For a group of non-dispersive body waves, the travel time from a hypocenter H to a receiver Δ_i is

$$T_i = \int_{H \rightarrow \Delta_i} u\,ds \tag{1}$$

where u is the reciprocal velocity, or slowness, and ds is the element of path length. Ignoring second order variations in T due to the assumed small change in integration path, a small change in the slowness $\delta u(z)$ results in a change in travel time of

$$\delta T_i = \int_{H \rightarrow \Delta_i} \delta u(z)\,ds \tag{2}$$

For the flat layered geometry used here we have for the i^{th} travel time observation with ray parameter p_i ,

$$\delta T_i = \int_L^0 \delta u(z) g_i(z) dz \tag{3}$$

where $g_i(z)$ depends on the source depth z_H as follows:

$$g_i(z) = \begin{cases} \dfrac{u(z)}{(u^2(z) - p_i^2)^{1/2}} & 0 < z \leq z_H \\ \dfrac{2u(z)}{(u^2(z) - p_i^2)^{1/2}} & z_H < z \leq \text{depth of ray bottom } (u = p_i) \\ 0 & z > \text{depth of ray bottom} \end{cases} \tag{4}$$

L is chosen in (3) as some depth below the deepest ray. Notice that the kernel $g_i(z)$ is singular at the turning point where $u = p_i$. This singularity can be removed through integrating by parts, yielding

$$\delta T_i = \delta u(0) G_i(0) - \int_L^0 \delta u'(z) G_i(z) dz \tag{5}$$

where

$$\delta u'(z) = \frac{d}{dz} \delta u(z) \quad \text{and} \quad G_i(z) = \int_l^z g_i(\xi) d\xi \ .$$

Discretizing the media into plane layers allows one to solve (5) for slowness gradient perturbations $\delta u'(z)$ and the surface slowness perturbation $\delta u(0)$ using standard linear inversion techniques. The gradients can then be integrated to yield a revised slowness, or equivalently, velocity model. The process can be continued until the root mean square (RMS) travel time residual is approximately equal to the standard error of the data. Practically speaking, the discretization of the media will remove the singularity in (5), and one could also solve for absolute slowness

perturbations with relative ease. The choice here of solving for the gradient is twofold. First, it is the change in velocity with depth rather than absolute values of velocity that governs the focussing of seismic energy and thus largely determines waveform characteristics. Secondly, the integration of the kernels $g_i(z)$ results in smoother solutions, which is important for stable iterations.

The above inversion for slowness gradient perturbations was carried out using a damped singular value decomposition algorithm (O'Connell, 1986). The damping provides additional stability in this typically unstable problem of velocity inversion. Undamped error and resolution estimates were made using $\mathbf{C} = \sigma^2\mathbf{V}\Lambda^{-2}\mathbf{V}^T$ and $\mathbf{R} = \mathbf{V}\mathbf{V}^T$, respectively, where $\mathbf{C}$ is the covariance matrix, $\mathbf{R}$ is the resolution matrix, and $\mathbf{G}=\mathbf{U}\Lambda\mathbf{V}^T$ is the standard singular value decomposition of the kernel matrix. σ here represents the smallest apriori variance in the data set, i.e., the instrumental timing errors alone. Because of the various uncertainties in picking arrival times, the equations in (5) were each weighted by their own uncertainties relative to σ. Inherent in this analysis is the tradeoff between error and resolution as a function of the number of singular values retained in the singular value decomposition. To achieve reasonable error, the smaller singular values must be disposed of at the price of poorer resolution. It is important to remember that $\mathbf{C}$ and $\mathbf{R}$ are only linear estimates for this non-linear problem. The pitfalls of ignoring the non-linear effect are discussed by Pavlis and Booker (1983).

The travel time data which were used in the inversion are listed in Tables 1a and 1b, which correspond to the source and receiver locations shown in Figures 1a and 1b. Three-component acceleration records were available for the events in Table 1a and the arrival times of P and S waves were measured off these records. S waves, assumed to have been generated at the site of the explosion, were picked off the transverse component of ground motion only when they

appeared particularly evident. Integrated accelerations aided in the selection. We estimate the overall accuracy of these S times to be approximatly 0.2 seconds. These data were supplemented with the P travel times listed in Table 1b, which were taken from the studies of Perret (1976) and Barker, et. al. (1985). Note that the events in Table 1b greatly extend the depth range of sources used in the inversion, which helps constrain the velocity. Also note that the depth to the water table for the events listed in Table 1a and 1b ranges between 580 km and 700 km, with an average of 650 m (Howard and Richardson, 1984). Thus, sources both above and below the water table have been included. To compensate for variations in topography, the shot depth used for a given shot was that relative to the average elevation of the stations recording the event. The actual depths of burial are given in Tables 1a and 1b. The total number of data used in the inversion was 72 P wave times and 20 S wave times.

The inversion method described above requires that a reasonably good initial estimate of the velocity model be available. The initial P wave model for the upper 700 m was obtained by averaging acoustic well log data derived from the shot reports of the events in Table 1a and from additional well data from Howard and Richardson (1984). The initial P wave model below 700 m was obtained from a average of previous models, making adjustments to reasonably match observed travel times as described above. Given the initial P model, the initial S wave model was obtained from the work by Carrol (1968), which relates shear velocity to compressional velocity through measurements of Young's modulus for Pahute Mesa and nearby Northern Yucca Flat volcanics. These initial models are shown in Figure 7.

For the purposes of the inversion, the media was discretized into 100 m thick layers down to a depth of 4 km. Unlike previous models which have characterized Silent Canyon Caldera by constant velocity layers, we have used a linear gradient velocity function. This should be more

consistent with the expected gradual increase in velocity due to sediment compaction. Such behavior is observed in the shallow well log data.

The results of the velocity inversion are shown in Figure 7 and Table 2. The inversions for the P and S models were done independently. It should be noted that the sharp features of the models are not resolvable by the travel time data. Rather, they are artifacts of the initial models. The P model converged in 3 iterations with an RMS residual of 0.096 seconds. The S model converged in only 2 iterations with an RMS residual of 0.112 seconds. Both solutions were obtained with damping values equal to approximatley 2% of the maximum singular value used in each inversion. The travel time residuals for these models are given in Table 1a and 1b. Additionally, Figure 5 shows the predicted P and S travel time curves for a shot buried 625 m averaging through the data from shots near that depth.

The initial P and S models were each revised down to 2.5 km. In the final models no rays in our data set penetrate below this depth and therefore the deeper velocity gradients remain unchanged from the initial model. The total number of singular values in the error and resolution analysis is thus 26, including one for the surface slowness. Of the 26, only 6 could be retained to achieve an acceptable amount of error for the P model. For the S model only 3 singular values could be kept. This small number is not surprising considering the larger errors of the S wave travel times. Figure 8a and 8b show the magnitude of the slowness gradient and its standard error for both models. The statistical fit is particularly good above 600 m. This is less than the typical depth of most of the shots used in this study, so there is an abundance of rays sampling above this depth. However, the lack of turning rays above 600 m results in poor vertical resolution here. This is shown rather well in Figures 9a and 9b where elements of the resolution matrix, **R**, for P and S wave slowness gradients are shaded according to their value. The poor vertical

resolution for the shallow P model is compensated by available well log data. Below 600 m the increased resolution of the P model trades off with the increased relative error. However, due to the lack of deeper shots, a smaller number of travel times, and larger reading errors, much of the S wave model remains poorly resolved.

Summary and Conclusions

The intent of this study has been to estimate an averaged one-dimensional velocity model for Silent Canyon Caldera. Our primary data set has been acoustic well log data and a relatively large set of travel times. These data have produced a one-dimensional averaged velocity model which fits the observed travel time data to within observational error. For comparison, our final model is shown in Figure 10 with four recently published models. A major difference between this and previous studies is the introduction of a continuous velocity model. The P wave velocity model of this study is slightly greater than previous models between depths of about 0.7 and 2 km, but this is compensated by the lower velocities at depths less than 0.3 km. The S wave velocity model is greater than the results of most other studies. Using our inversion approach, a one-dimensional model could be even better constrained with a broader depth distribution of sources and more recorded travel times, particularly those of S waves. Though a one dimensional model may satisfy travel time data to within acceptable error, amplitude, waveform, and geologic data indicate that lateral heterogeneity within Silent Canyon Caldera is significant. Given the desire for unequivocal descriptions of nuclear sources, a more detailed investigation of the three dimensional seismic structure of the caldera is certainly warranted by the above discussions.

Acknowledgments

We would like to thank Dan O'Connell for the use of his travel time inversion program as well as for his helpful comments. This research was supported by the Defense Advanced Research Projects Agency and was monitored by the Air Force Geophysics Laboratory under Contract F19628-85-K-0025 and through U. S. Department of Energy Contract No. DE-AC03-76SF00098.

References

Backus, G. and F. Gilbert (1969). Constructing P-velocity models to fit restricted sets of travel-time data, *Bull. Seism. Soc. Am.* **59**, 1407-1414.

Barker, J. S., S. H. Hartzell, L. J. Burdick, and D. V. Helmberger (1985). Determination of effective source functions and measurement of seismic yields from underground nuclear explosions at Pahute Mesa by modeling near-field records, *Final Technical Report: WCCP-R-85-02* , Woodward-Clyde Consultants, Pasadena, CA.

Carrol, R. D. (1966). Preliminary interpretation of geophysical logs, UE20f, Pahute Mesa, Nevada Test Site, *Technical Letter: Special Studies-I-37, Supplement 1, U. S. Geol. Survey Open File Report* , 7 p.

Hamilton, R. M. and J. H. Healy (1969). Aftershocks of the BENHAM nuclear explosion, *Bull. Seism. Soc. Am.* **59** , 2271-2281.

Hartzell, S. H., L. J. Burdick, and T. Lay, (1983). Effective source functions for Pahute Mesa nuclear tests, *Final Technical Report WCCP-R-83-3, Woodward-Clyde Consultants, Pasadena, CA.*

Healy, D. L. (1968). Application of gravity data to geologic problems at Nevada Test Site, *Geol. Soc. Am. Memoir* **110** , 147-156

Helmberger, D. V. and D. M. Hadley (1981). Seismic source functions and attenuation from local and teleseismic observations of NTS events JORUM and HANDLEY, *Bull. Seism. Soc. Am.* **71** , 51-68.

Howard, N. W. and W. Richardson (1984). Selected event data, *Reference UCID 18542-84 (CFRD)* , Lawrence Livermore Laboratory.

Noble, D. C., K. A. Sargent, H. H. Mehnert, E. B. Ekren, and F. M. Byers (1968). Silent Canyon Volcanic Center. *Geol. Soc. Am. Memoir* **110** , 65-76.

O'Connell, D. R. (1986). Seismic velocity structure and microearthquake source properties at The Geysers, California, Geothermal Area, *Ph.D. Thesis* , Univesity of California, Berkeley, California.

Orkild, F. M., F. M. Byers, D. L. Hoover, and K. A. Sargent (1968). Subsurface geology of Silent Canyon Caldera, Nevada Test Site, Nevada, *Geol. Soc. Am. Memoir* **110** , 77-86.

Pavlis, G. L. and J. R. Booker (1980). The mixed discrete-continuous inverse problem: Application to the simultaneous determination of earthquake hypocenters and velocity structure, *J. Geophys. Res.* **85** , 4801-4810.

Pavlis, G. L. and J. R. Booker (1983). A study of the importance of nonlinearity in the inversion of earthquake arrival time data for velocity structure, *J. Geophys. Res.* **88** , 5047-5055.

Perret, W. R. (1976). Surface motions induced by nuclear explosions beneath Pahute Mesa, *Report SC-RR-71-0068* , Sandia Laboratories, Albequerque, NM.

Stump, B. W. and L. R. Johnson (1984). Near-field source characterization of contained nuclear explosions in tuff, *Bull. Seism. Soc. Am.* **74** , 1-26.

Taner, M. T. and F. Koeler (1969). Velocity spectra- digital computor derivation and applications of velocity functions, *Geophysics* **34** , 859-881.

Taylor, S. R. (1983). Three-dimensional crust and upper mantle structure at the Nevada Test Site, *J. Geophys. Res.* **88** , 2220-2232.

TABLE 1a

TRAVEL TIMES AND RESIDUALS

EVENT	DEPTH (m)	STA.	Δ (km)	P TIME (sec)	ΔT_P (sec)	S TIME (sec)	ΔT_S (sec)
CHANCELLOR	625	10	1.85	0.790	0.07	1.25	0.01
		3	2.11	0.786	-0.01	1.40	0.03
		2	2.67	1.053	0.10	1.60	-0.05
		0	3.09	1.027	-0.04	-	-
		5	4.48	1.328	-0.13	2.30	-0.27
		4	5.52	1.631	-0.11	-	-
		9	5.60	1.812	0.05	-	-
		6	6.03	1.696	-0.17	-	-
		1	9.35	2.655	0.00	-	-
		7	9.82	2.540	-0.22	-	-
		8	10.82	3.103	0.12	5.67	0.04
COLWICK	633	4	4.94	1.617	0.02	2.90	0.08
		1	4.94	1.627	0.03	2.92	0.10
		2	4.94	1.662	0.07	3.00	[illegible]
		7	5.02	1.677	0.06	3.04	0.17
		8	5.03	1.841	0.22	3.02	0.15
		6	5.11	1.712	0.07	3.08	0.17
		9	5.11	1.717	0.08	3.05	0.14
		3	5.29	1.737	0.05	3.15	0.15
EMMENTHAL	576	4	0.51	0.289	-0.04	0.32	0.00
		6	0.76	0.354	-0.05	0.35	0.02
		3	0.89	0.424	-0.02	0.42	0.04
FARM	689	4	4.22	1.332	-0.04	-	-
		6	4.72	1.252	-0.26	-	-
		5	6.38	1.796	-0.16	-	-
		2	9.73	2.605	-0.18	-	-
HARZER	637	4	3.43	1.15	-0.02	-	-
		2	3.52	1.03	-0.16	-	-
		1	4.65	1.39	-0.11	-	-
		6	5.61	1.85	0.09	-	-
		8	5.78	1.87	0.06	-	-
		5	6.62	2.00	-0.03	-	-
PIPKIN	624	1	2.71	1.05	0.10	-	-
		2	5.72	2.07	0.28	-	-
		3	7.69	2.56	0.28	-	-
SERPA (+)	630	9	8.63	-	-	4.65	-0.01
		7	8.79	-	-	4.70	-0.04
		6	8.87	-	-	4.75	-0.02
		5	8.95	-	-	4.80	-0.01

+ Gross timing errors. S times picked after P times set to predicted times.

TABLE 1b

TRAVEL TIMES AND RESIDUALS

EVENT	DEPTH (m)	STA.	Δ (km)	P TIME (sec)	ΔT_P (sec)
BOXCAR (*)	1166	1	0.300	0.47	0.04
		3	0.91	0.56	0.05
		8	2.40	0.90	0.03
		12	3.81	1.26	0.01
		16	4.87	1.51	-0.01
		24	7.27	2.10	-0.01
		34	10.37	2.92	0.13
GREELY (*)	1216	1	0.015	0.430	0.00
		2	0.61	0.480	0.01
		3	1.22	0.600	0.01
HALFBEAK (*)	819	1	0.015	0.330	0.01
		2	0.46	0.410	0.05
		3	0.91	0.490	0.03
		4	1.37	0.640	0.06
		7	2.13	0.740	-0.05
		5	2.13	0.820	0.03
		8	2.28	0.880	0.04
		6	3.05	1.040	-0.01
INLET (#)	819	E	0.01	0.31	-0.01
		W	0.01	0.31	-0.01
		3	0.41	0.36	0.01
		4	0.82	0.44	0.00
		5	1.63	0.59	-0.06
		6	3.27	1.03	-0.08
		7	6.53	1.99	0.02
MAST (#)	911	Z	0.01	0.36	0.02
		2	0.46	0.40	0.02
		3	0.91	0.51	0.04
		4	1.82	0.71	0.00
		5	3.65	1.15	-0.06
		6	5.47	1.56	-0.13
		7	7.30	2.03	-0.11
SCOTCH (*)	977	1	0.02	0.41	0.05
		2	1.21	0.64	0.08
		3	2.29	0.98	0.14
		3A	4.13	1.38	0.04
		4	6.06	1.89	0.05

* Times from Perret (1976).

\# Times from Barker, et. al. (1985).

TABLE 2

P AND S VELOCITY

DEPTH (km)	P VELOCITY (km/sec)	S VELOCITY (km/sec)
0.00	1.50	0.99
0.10	1.90	1.24
0.20	2.30	1.47
0.30	2.51	1.56
0.40	2.71	1.64
0.50	2.92	1.72
0.60	3.13	1.80
0.70	3.55	1.96
0.80	3.55	1.96
0.90	3.65	1.97
1.00	3.70	1.98
1.10	3.76	2.00
1.20	3.82	2.02
1.30	3.87	2.04
1.40	3.92	2.06
1.50	4.00	2.09
1.60	4.07	2.12
1.70	4.16	2.15
1.80	4.24	2.19
1.90	4.32	2.22
2.00	4.40	2.25
2.10	4.47	2.27
2.20	4.52	2.30
2.30	4.56	2.33
2.40	4.58	2.36
2.50	4.62	2.38

Figure Captions

Figure 1a. Explosion sites (open circles) and respective recording sites (filled circles) for shots near 625 m depth at Pahute Mesa of the Nevada Test Site. See Table 1a.

Figure 1b. Additional explosion sites (open circles) and respective recording sites (filled circles). See Table 1b.

Figure 2. Vertical accelerations from shots shown in Figure 1a. Shot depths are near 625 m.

Figure 3. Radial accelerations from shots shown in Figure 1a. Shot depths are near 625 m.

Figure 4. Transverse accelerations from shots shown in Figure 1a. Shot depths are near 625 m.

Figure 5. Measured P wave and S wave travel times for shots buried near 625 m. Predicted times for a shot buried 625 m, as determined from our final model, are given by the solid curves.

Figure 6. Ratio of vertical to radial P wave acceleration for shots buried near 625 m. Amplitudes were measured off the first quarter cycle.

Figure 7. Initial and revised velocity models. No constraints are placed on the models below 2.5 km, thus the deeper velocity gradients remain unchanged from the initial model.

Figure 8a. Final slowness gradient and standard error (diagonal elements of the covariance matrix $\mathbf{C}$) for the P wave model. The slowness gradient is actually negative ; it's absolute value is plotted.

Figure 8b. Same as Fig. 8a., but for S wave model.

Figure 9a. Elements of the resolving matrix, $\mathbf{R}$, for the P wave model. The values are are divided into six levels and shaded with a corresponding density. The upgoing diagonals signify negative values, indicative of side lobes. The first row and column pertain to the value of surface slowness.

Figure 9b. Same as Fig. 9a., but for S wave model.

Figure 10. Final P and S wave velocity models plotted with recently published models.

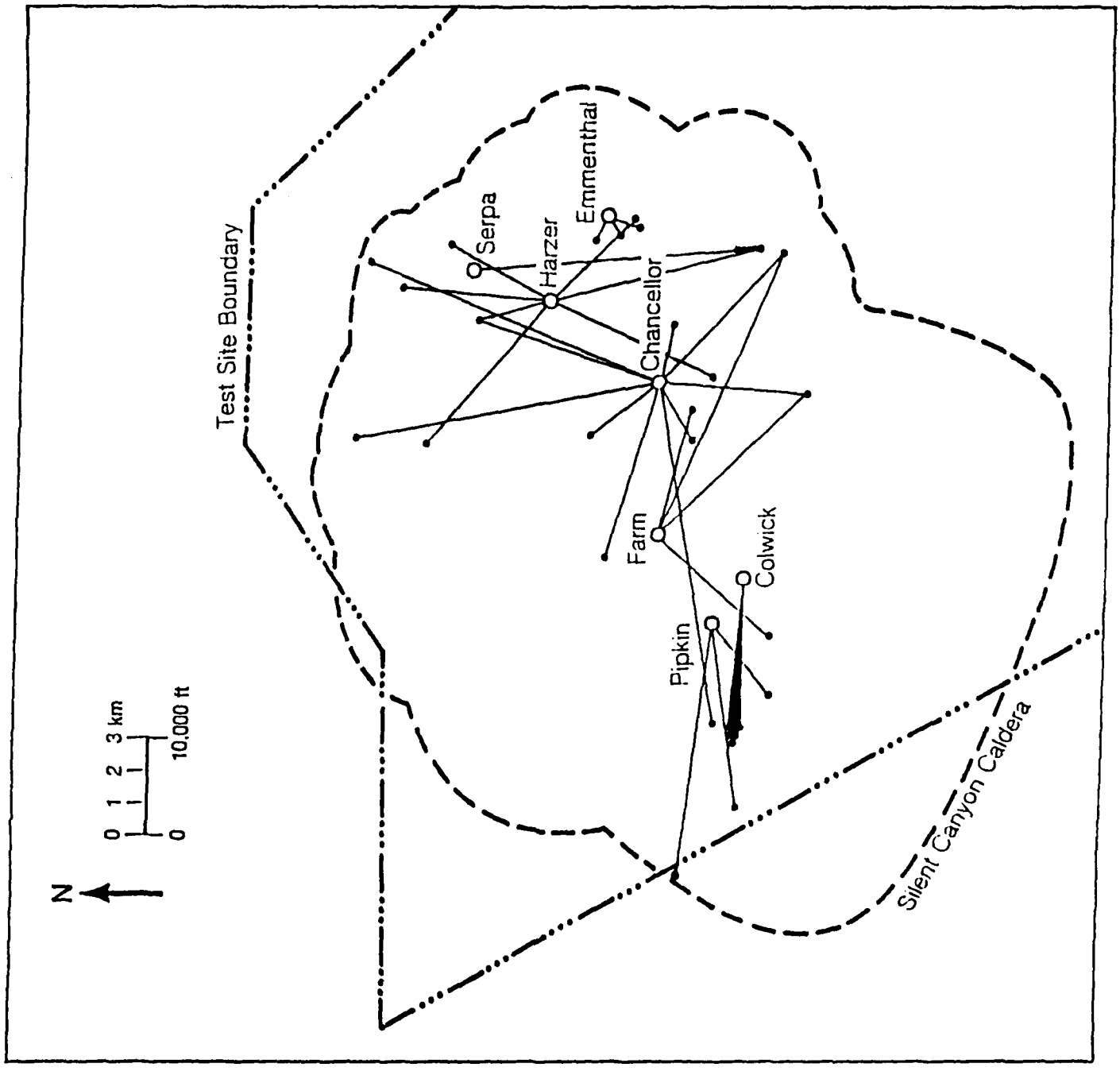

Figure 1a. Explosion sites (open circles) and respective recording sites (filled circles) for shots near 625 m depth at Pahute Mesa of the Nevada Test Site. See Table 1a.

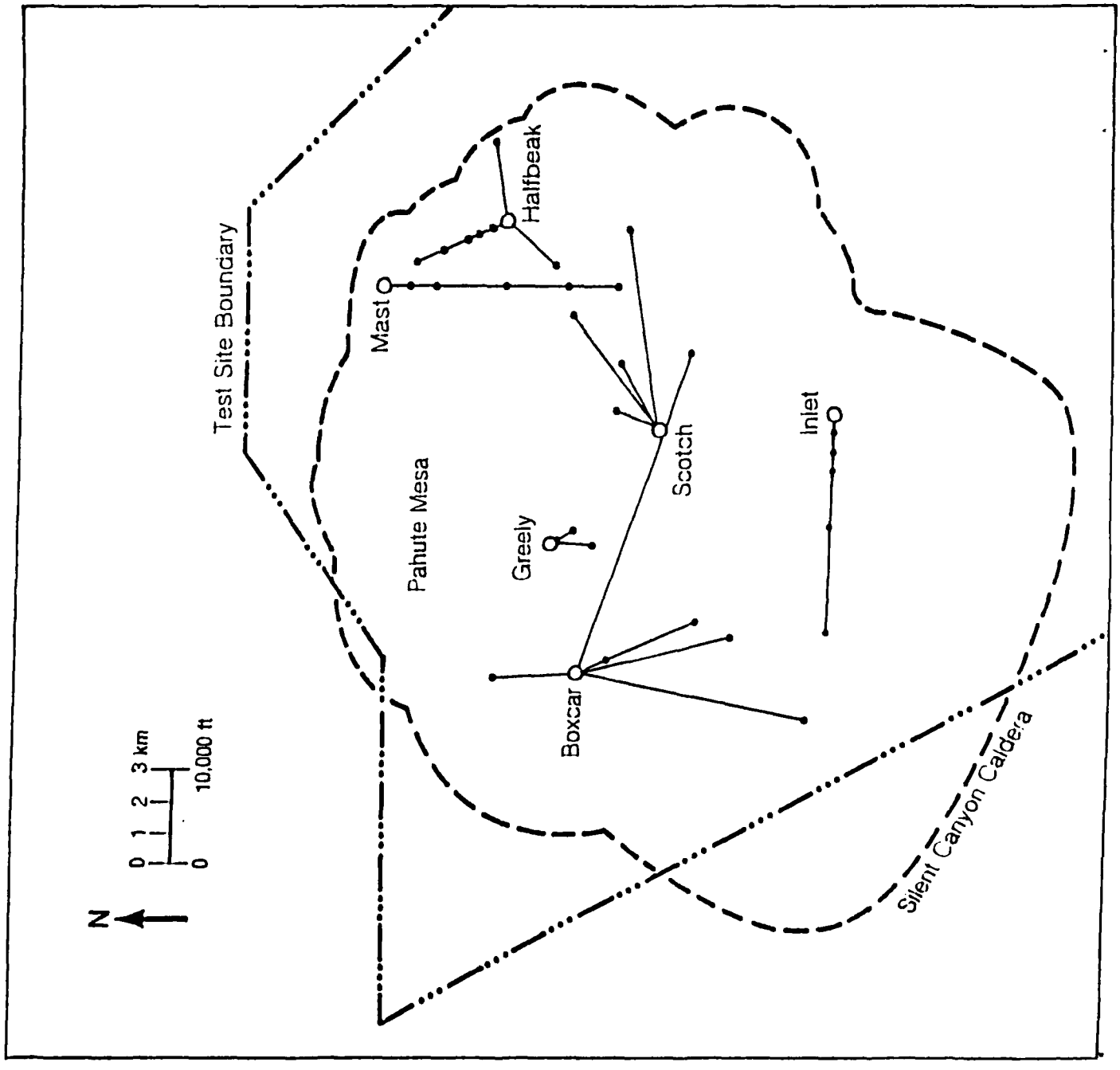

Figure 1b. Additional explosion sites (open circles) and respective recording sites (filled circles). See Table 1b.

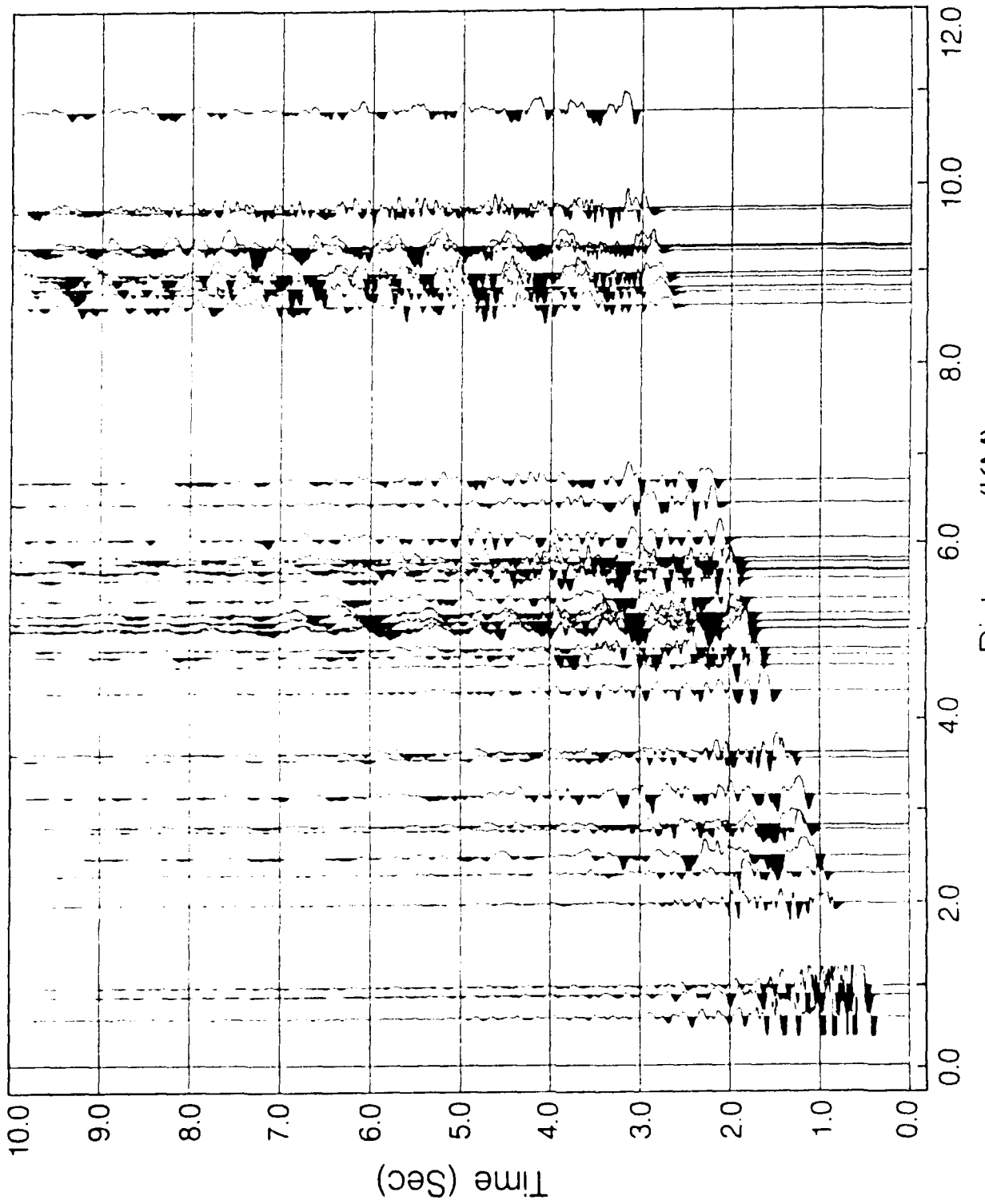

Figure 2. Vertical accelerations from shots shown in Figure 1a. Shot depths are near 625 m.

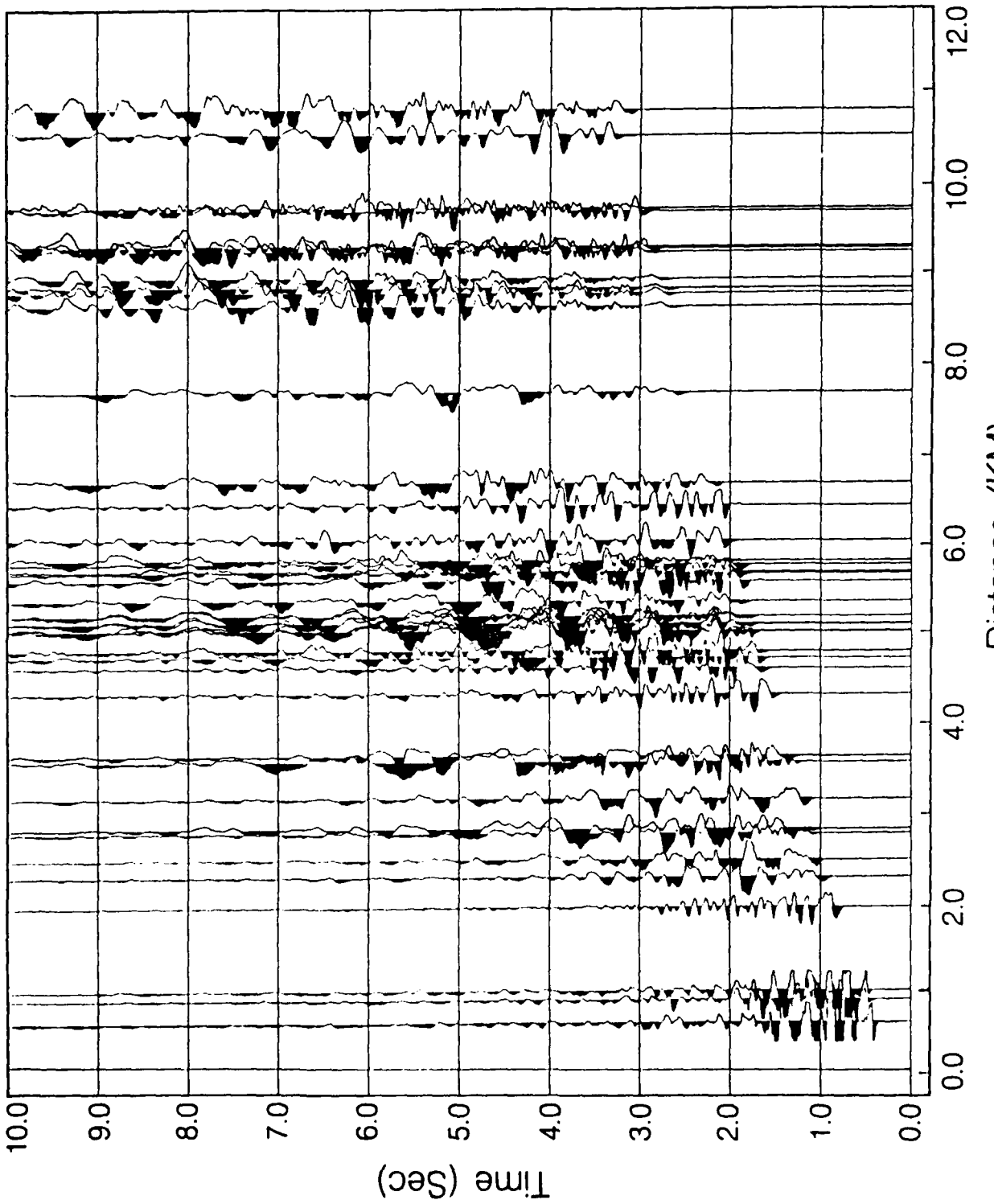

Figure 3. Radial accelerations from shots shown in Figure 1a. Shot depths are near 625 m.

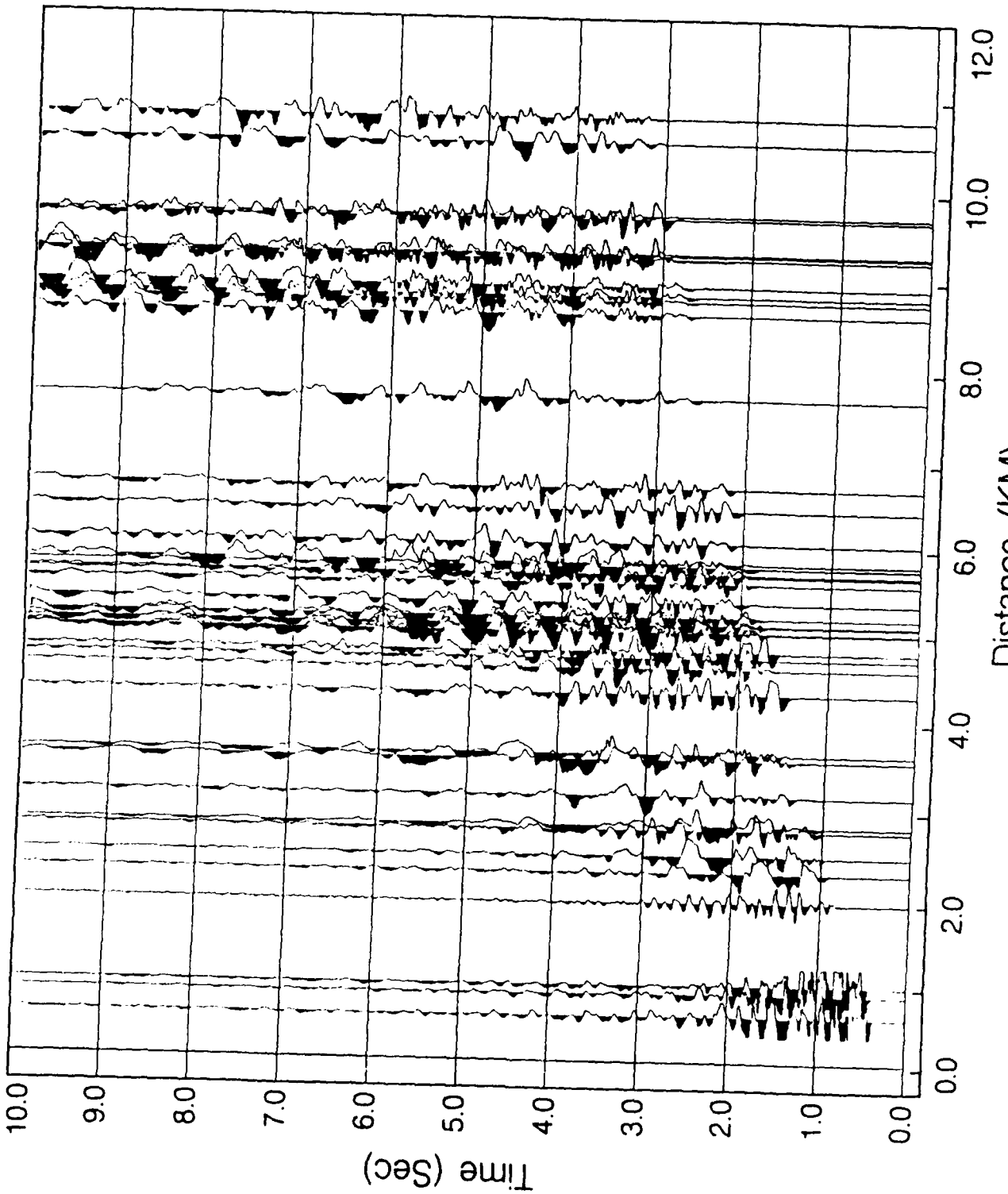

Figure 4. Transverse accelerations from shots shown in Figure 1a. Shot depths are near 625
m

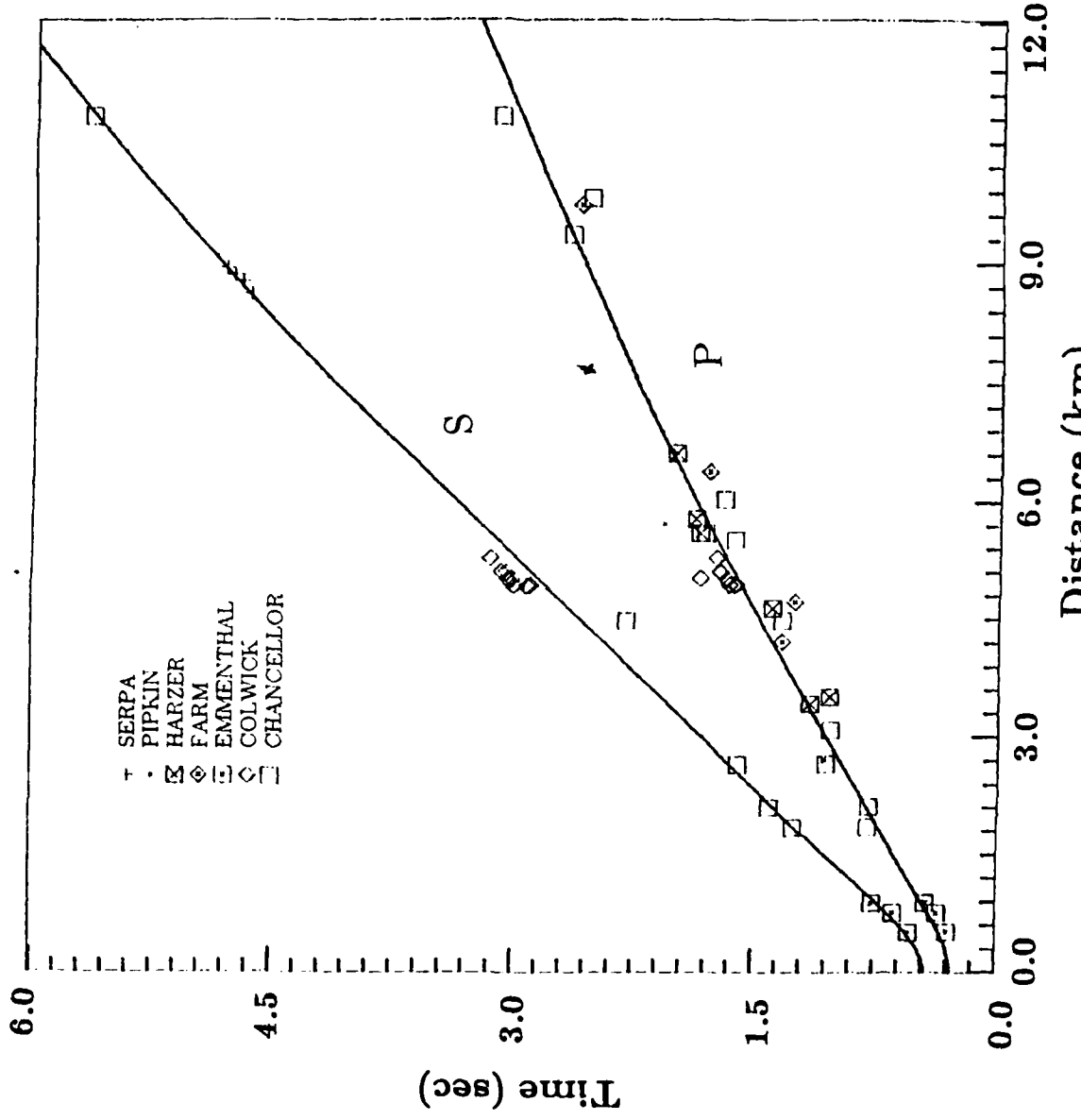

Figure 5. Measured P wave and S wave travel times for shots buried near 625 m. Predicted times for a shot buried 625 m, as determined from our final model, are given by the solid curves.

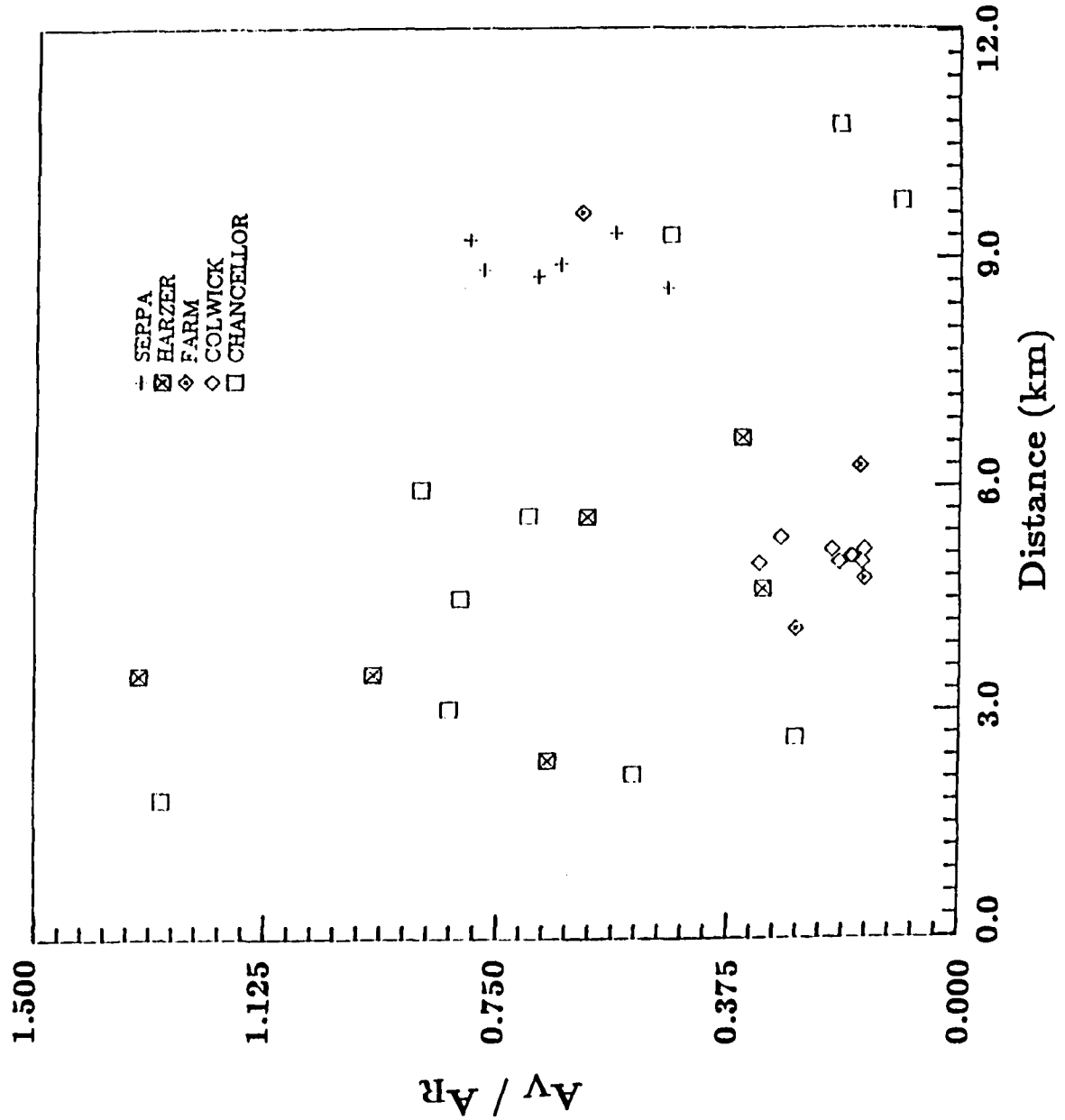

Figure 6. Ratio of vertical to radial P wave acceleration for shots buried near 625 m. Amplitudes were measured off the first quarter cycle.

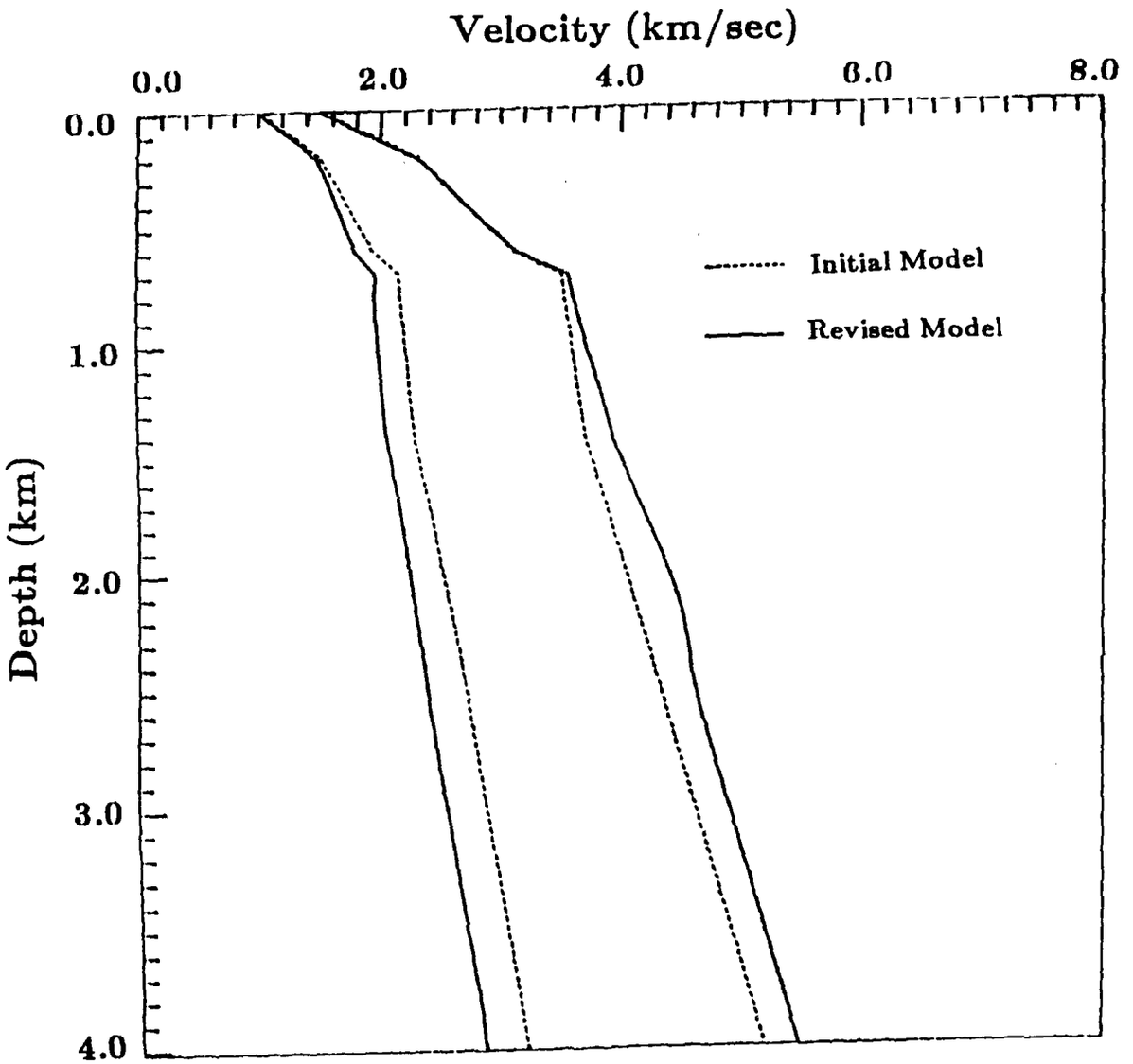

Figure 7. *Initial and revised velocity models.* No constraints are placed on the models below 2.5 km, thus the deeper velocity gradients remain unchanged from the initial model.

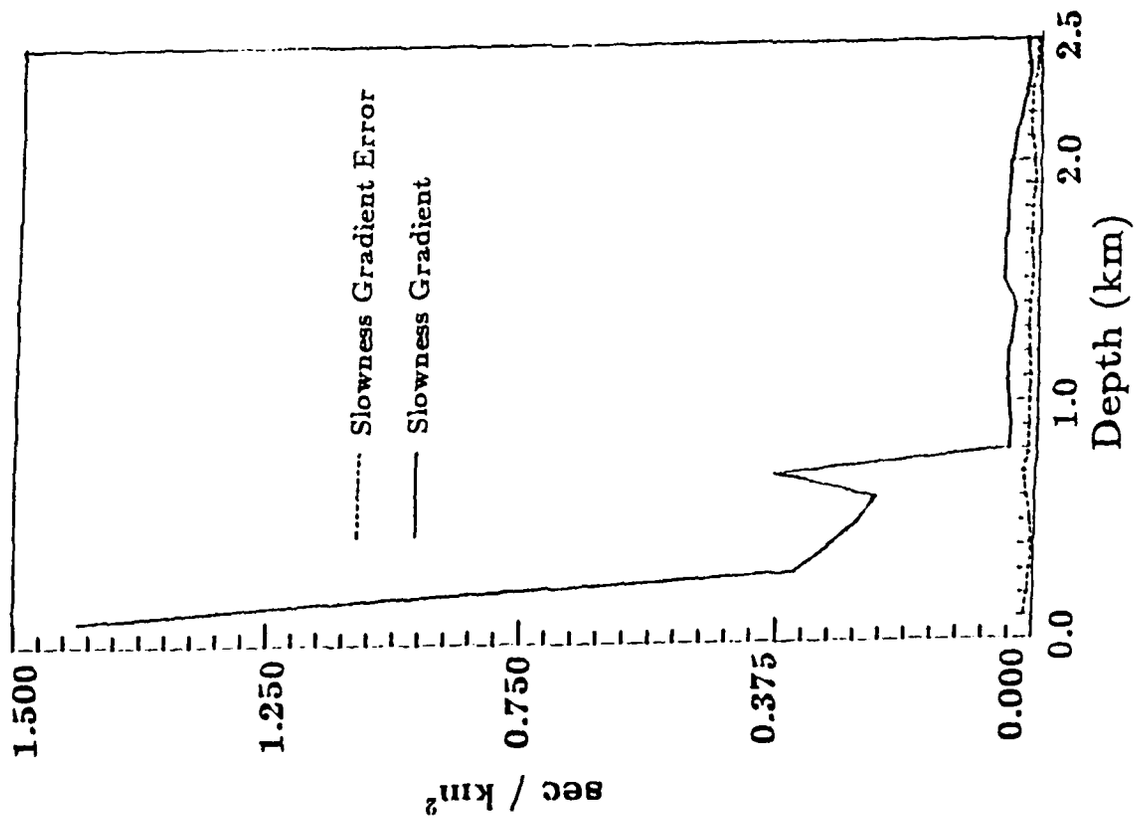

Figure 8a. Final slowness gradient and standard error (diagonal elements of the covariance matrix $\mathbf{C}$) for the P wave model. The slowness gradient is actually negative ; it's absolute value is plotted.

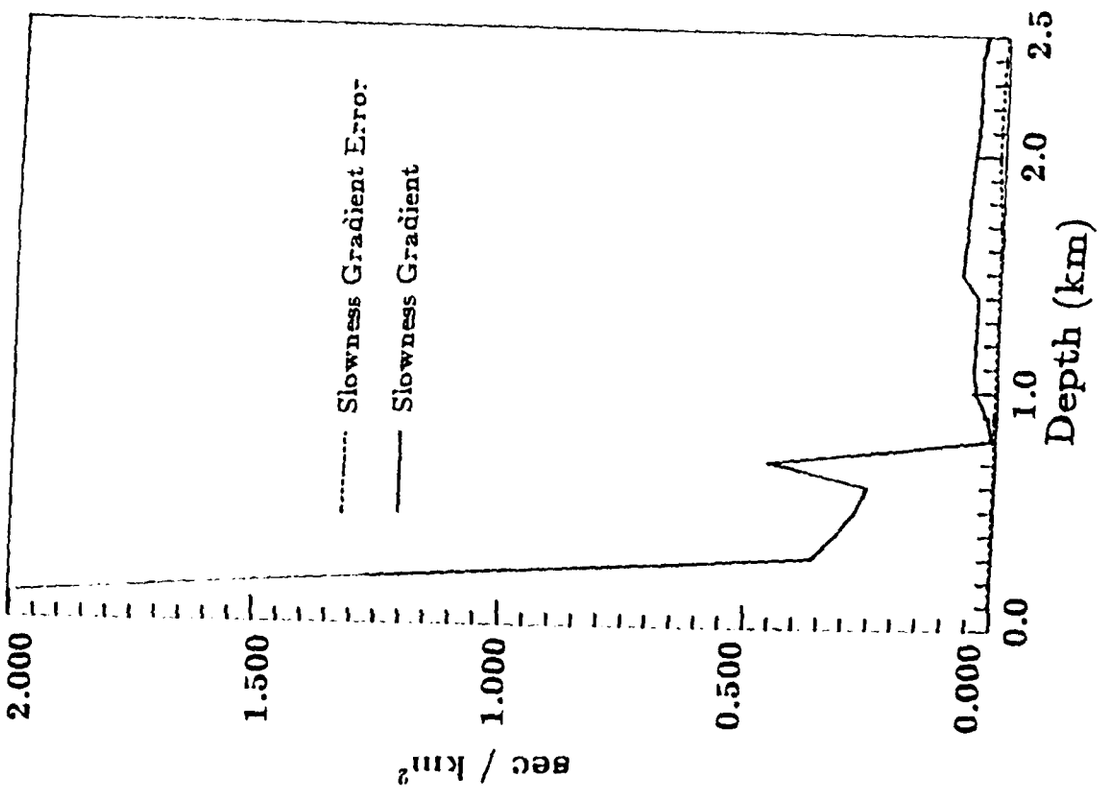

Figure 8b. Same as Fig. 8a., but for S wave model.

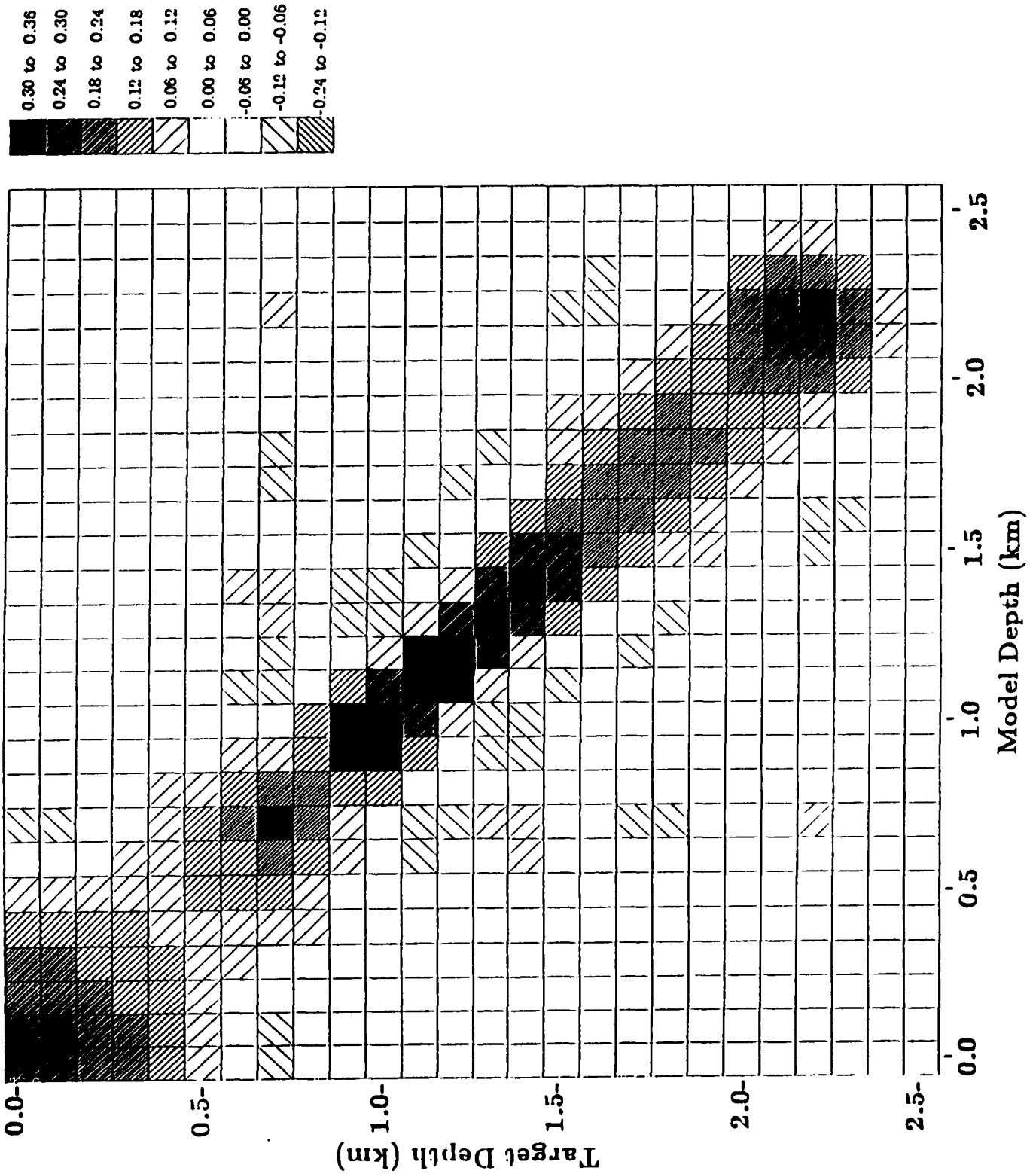

Figure 9a. Elements of the resolving matrix, R , for the P wave model. The values are are divided into six levels and shaded with a corresponding density. The upgoing diagonals signify negative values, indicative of side lobes. The first row and column pertain to the value of surface slowness.

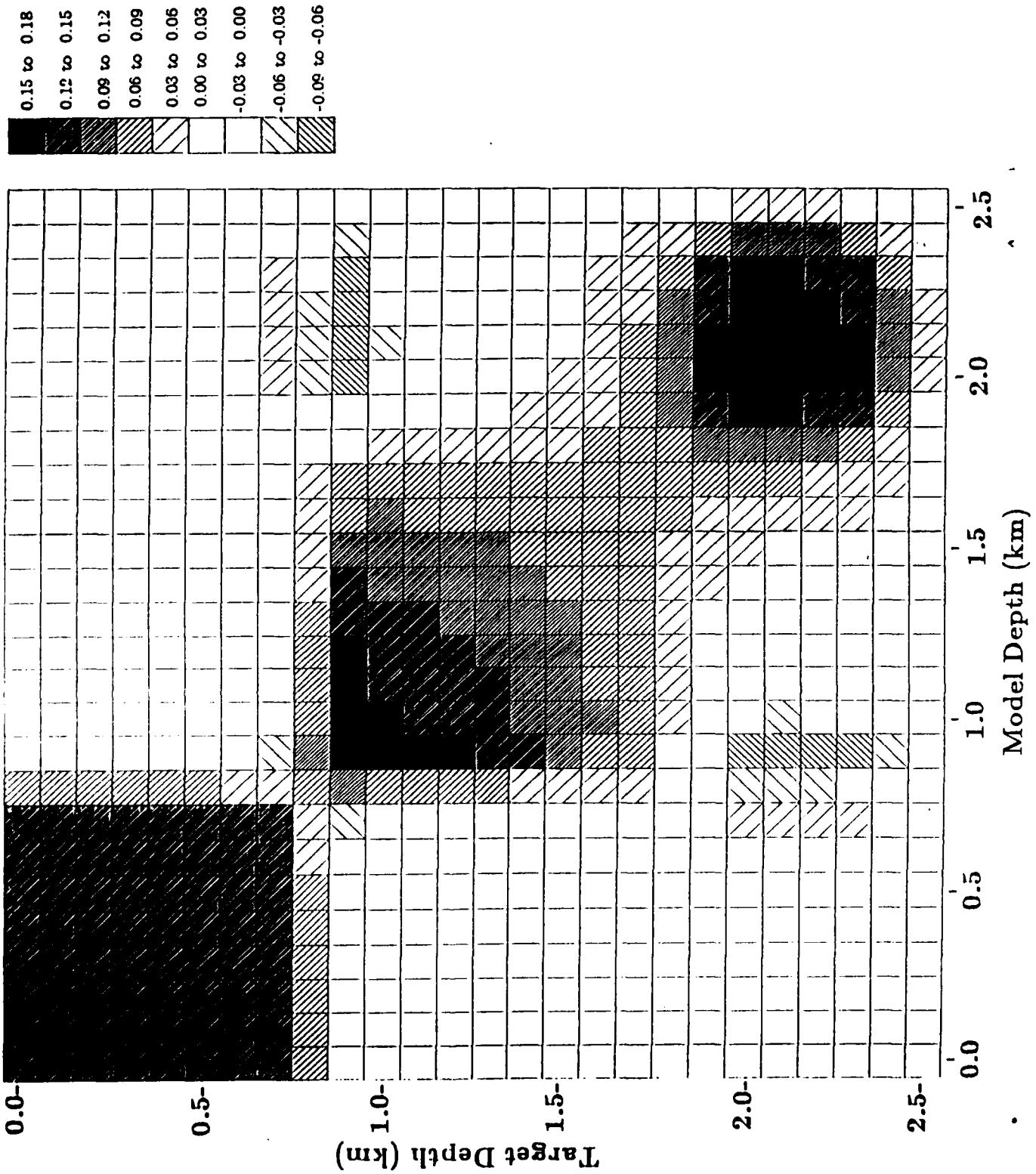

Figure 9b. Same as Fig. 9a., but for S wave model.

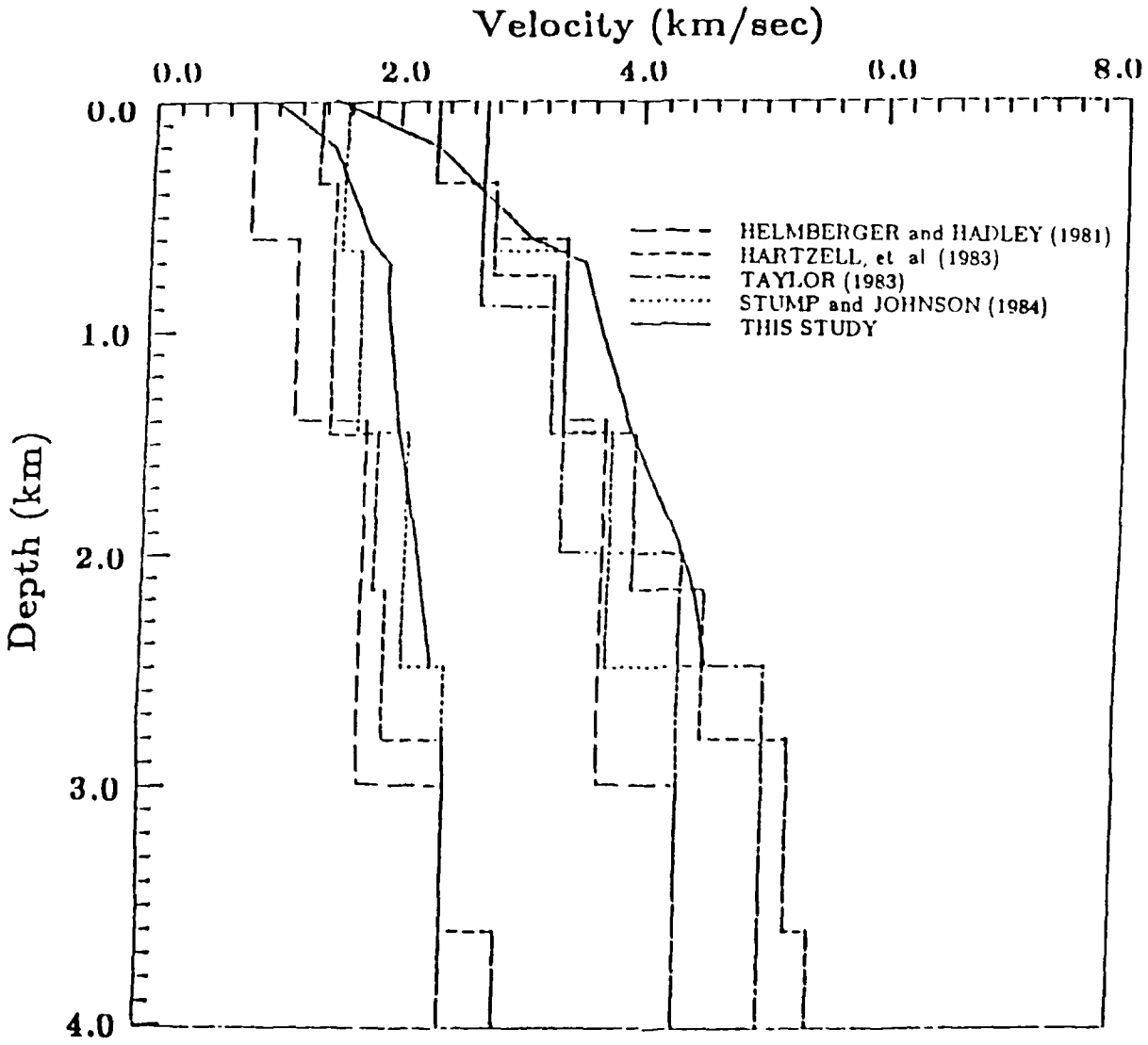

Figure 10. Final P and S wave velocity models plotted with recently published models.

END

10-86

DTIC